JGR Planets

RESEARCH ARTICLE
10.1029/2019JE006241

Key Points:
- Antarctic micrometeorite collections are time-averaged windows of the cosmic dust flux, in terms of mass, size and composition
- The near-Earth cosmic dust complex has a bimodal size distribution, as inferred from micrometeorite collections at the Earth's surface
- The average flux of cosmic dust to Earth over the Quaternary, inferred from the TAM65 trap lies between ~800 and 2,300 t/yr

Correspondence to:
M. D. Suttle,
martindavid.suttle@dst.unipi.it

Citation:
Suttle, M. D., & Folco, L. (2020). The extraterrestrial dust flux: Size distribution and mass contribution estimates inferred from the Transantarctic Mountain (TAM) micrometeorite collection. *Journal of Geophysical Research: Planets*, *125*, e2019JE006241. https://doi.org/10.1029/2019JE006241

Received 15 OCT 2019
Accepted 9 JAN 2020
Accepted article online 30 JAN 2020

The Extraterrestrial Dust Flux: Size Distribution and Mass Contribution Estimates Inferred From the Transantarctic Mountains (TAM) Micrometeorite Collection

M. D. Suttle[1,2] **and L. Folco**[1,3]

[1]Dipartimento di Scienze della Terra, Università di Pisa, Pisa, Italy, [2]Planetary Materials Group, Department of Earth Sciences, Natural History Museum, London, UK, [3]Centro per l'Integrazione della Strumentazione dell'Università di Pisa, Pisa, Italy

Abstract This study explores the long-duration (0.8–2.3 Ma), time-averaged micrometeorite flux (mass and size distribution) reaching Earth, as recorded by the Transantarctic Mountains (TAM) micrometeorite collection. We investigate a single sediment trap (TAM65), performing an exhaustive recovery and characterization effort and identifying 1,643 micrometeorites (between 100 and 2,000 μm). Approximately 7% of particles are unmelted or scoriaceous, of which 75% are fine-grained. Among cosmic spherules, 95.6% are silicate-dominated S-types, and further subdivided into porphyritic (16.9%), barred olivine (19.9%), cryptocrystalline (51.6%), and vitreous (7.5%). Our (rank)-size distribution is fit against a power law with a slope of −3.9 ($R^2 = 0.98$) over the size range 200–700 μm. However, the distribution is also bimodal, with peaks centered at ~145 and ~250 μm. Remarkably similar peak positions are observed in the Larkman Nunatak data. These observations suggest that the micrometeorite flux is composed of multiple dust sources with distinct size distributions. In terms of mass, the TAM65 trap contains 1.77 g of extraterrestrial dust in 15 kg of sediment (<5 mm). Upscaling to a global annual estimate gives 1,555 (±753) t/year—consistent with previous micrometeorite abundance estimates and almost identical to the South Pole Water Well estimate (~1,600 t/year), potentially indicating minimal variation in the background cosmic dust flux over the Quaternary. The greatest uncertainty in our mass flux calculation is the accumulation window. A minimum age (0.8 Ma) is robustly inferred from the presence of Australasian microtektites, while the upper age (~2.3 Ma) is loosely constrained based on ^{10}Be exposure dating of glacial surfaces at Roberts Butte (6 km from our sample site).

Plain Language Summary Each year the Earth collects large amounts of extraterrestrial material, with a significant fraction in the form of submillimeter cosmic dust, originating from asteroids and comets. This material adds elements such as nickel and sodium to the Earth's atmosphere, which effect the ionosphere. In the past, cosmic dust may have also played an important role in the origin of life as well as potentially contributing to mass extinction events. Here we examine an ancient (>0.8-million-year-old) micrometeorite collection found among the Transantarctic Mountains. We estimate the quantity of cosmic dust falling to Earth over this time period to be between (approximately) 800 and 2,300 tons per year. In addition, we demonstrate that the cosmic dust flux contains at least two dominant sources with different size distributions. This could reflect the relative contributions from inner solar system asteroids and outer solar system comets.

1. Introduction

The flux of extraterrestrial material falling to Earth is dominated by interplanetary (or cosmic) dust particles —termed micrometeorites (Genge et al., 2008; Zolensky et al., 2006). This continual addition affects the Earth's atmosphere through the deposition metallic ion layers (e.g., Ni layers; Bones et al., 2019) and may have rare but significant effects on the Earth's climate and biosphere—for example, periods of enhanced dust flux could disrupt climatic stability, as may have occurred during the end Ordovician, where the breakup of the L-chondrite parent asteroid led to dramatic increases in the quantity of cosmic dust arriving on Earth. This may have been responsible for the onset of icehouse conditions (Schmitz et al., 2019).

Estimates of the micrometeorite flux falling today and over the Quaternary—in terms of mass, composition, and origin, are generally limited to the data from collections with relatively short accumulation windows

(≤50 ka old) and based on micrometeorite populations with small average sizes (typically 200–400 μm; Table 1). Global flux estimates, determined from micrometeorites collections, vary widely, over 3 orders of magnitude from hundreds to thousands tons per year (e.g., Prasad et al., 2013; Taylor et al., 1998, 2000; Yada et al., 2004). Whether this uncertainty is due to real variation in flux over short time scales or due to collection biases is not yet clear (Genge et al., 2017).

In contrast, the Transantarctic Mountains (TAM) micrometeorite collection samples the cosmic dust flux over significantly longer time scales (>1 Ma), contains many thousands of individual particles up to 3 mm in size and boasts an abundance of otherwise rare unmelted and giant micrometeorites (Folco et al., 2008; Rochette et al., 2008; Suavet et al., 2009, 2011; van Ginneken et al., 2012; Suttle et al., 2019). These micrometeorites are found trapped in loose sediments, accumulated on bedrocks with (^{10}Be exposure) ages attesting to ancient glacially eroded, granitic surfaces, preserved in the Victoria Land TAM (Rochette et al., 2008; Welten et al., 2008).

The TAM micrometeorite collection provides a unique opportunity to obtain a time-averaged estimate of the flux of micrometeorites over the recent geological past (both qualitative [parentage] and quantitative [amount]). Looking to the future, this collection therefore has the potential to act as a ground-truth for a number of timely and controversial issues in Earth and Planetary Science; they include the following:

1. The composition of the inner Solar System's interplanetary dust complex (Cordier & Folco, 2014);
2. The geological investigation of otherwise unsampled bodies, not only asteroids, but comets and potentially planets and their satellites as well (Genge et al., 2008; Jolliff et al., 1993; Noguchi et al., 2015; Suavet et al., 2010);
3. The dynamical evolution of the zodiacal cloud (Nishiizumi et al., 1995; Nesvorný et al., 2006, 2010);
4. The contribution of extraterrestrial matter to the Earth's geochemical budget (Peucker-Ehrenbrink, 1996); and
5. The identification of periods with enhanced dust flux associated with catastrophic collisions and asteroid family formation within the Main Asteroid Belt (or through increased cometary activity). Such periods are inferred from cosmic dust abundance peaks preserved in the geological record (e.g., Schmitz et al., 2019; Suttle & Genge, 2017).

Here we provide a comprehensive characterization of the TAM micrometeorite accumulation dynamics and resulting micrometeorite collection. This is achieved through the case study of a single (loose) sediment trap (labeled TAM65), located at the top of Miller Butte, a glacially eroded nunatak within the Victoria Land TAM, Antarctica (Figures 1–3). We provide size distribution data for this trap, as well as data on the size distribution by textural subtype, the relative abundance of unmelted micrometeorites, and a clearly explained calculation of the mass flux of cosmic dust as inferred from our collection.

2. Geological Setting of the TAM65 Micrometeorite Sediment Trap and Collection Procedures

The micrometeorite collection studied in this work is from a single trap labeled TAM65. This was identified and sampled on the summit plateau of Miller Butte (72°42′03.30″S, 160°15′34.20″E), Victoria Land Transantarctic Mountains (Figure 1a), during the XXXVIII (2017–2018) Italian Antarctic Campaign of the Programma Nazionale delle Ricerche in Antartide. Miller Butte is a large arrowhead-shaped rock butte with a summit plateau extending for about ~4 km^2 in the Outback Nunatak region, in the inland catchment of the Rennick Glacier (Figure 1b). The butte, culminating at 2,610 m above sea level, is virtually ice-free and consists of felsic granitoids belonging to the Paleozoic Granite Harbour Intrusive Complex (Gunn &Warren, 1962; GANOVEX III, 1987). This projects for as much as 600 m above the ice sheet descending eastward from the Polar Plateau toward the upper sector of the outlet Rennick Glacier (e.g., D'Orazio et al., 2006; Folco et al., 2002).

The summit plateau of Miller Butte is a gently undulated, subhorizontal surface subparallel to one of the three sets of joints linked to the emplacement and cooling of the igneous body (Figure 2). On this surface, large areas of barren glacial polish (glossy bedrock glacial erosion surfaces), with local striated patterns and streamlined features, alternate to blockfields produced by the erosion of the jointed granitic body. The summit plateau is the remnant of a peneplaned surface produced by the overriding of the East

Table 1
Statistical Data and Site Metadata From Established Micrometeorite Collections: A Comparison of Population Statistics, Age, Site Productivity, and Inferences About the Cosmic Dust Flux

Collection	TAM (Yada & Kojima, 2000)	Larkman	Widerøfjellet Mountain	Greenland	DFWW	SPWW	Cap Prud'homme	CONCORDIA	Urban	Indian Ocean
Reference	*This study*	Genge et al. (2018) and Suttle et al. (2015)	Goderis et al. (2019)	Maurette et al. (1987, 1989, 1991)	Nakamura et al. (1999), Yada et al. (2000, 2004), and Terada et al. (2001)	Taylor et al. (1998, 2000, 2007, 2012)	Genge et al. (2018) and Suttle (unpublished)	Duprat et al. (2001, 2004, 2007) and Dobrica et al. (2010)	Genge et al. (2017)	Prasad et al. (2013, 2018)
Location	Antarctic			Greenland	Antarctic			Antarctic	Europe	Indian Ocean
Type	Weathering trap(s)	Moraine	Weathering traps	Cryconite	Blue Ice			Snow	Loose sediments (roof tops)	Deep-sea
Time window	≥2.3 Ma	~800 ka	<3 Ma	2000–3000 years	27–33 ka	~450 years (1100–1500 AD)	≪1000 years	20 years (1950–1970)	≪50 years	~50,000 years
Size fraction investigated (μm)	100–1500	60–450	0–3000	50–300	10–238 and 40–900	50–700	50–150	30–1000	100–800	50–750
No. of CSs studied	1643	634	2099	2560	942	1588	550	444	500	481
UMM/CSs ratio	0.07	0.01	0.05	0.43	0.56	0.02–0.97[a]	0.5	0.89–1.3	0	0.41
UMM: Fg/Cg ratio	~3.5	No data	No data	No data	No data	No data	No data	No data	No data	No data
Size distribution: value	**−3.92**	−5.34	−4.4 ± 0.2		−3.6 ± 0.4	−5.2 ± 0.5				−3.93
Size distribution: range fitted (μm)	200–700	210–330	300–800		50–200	200–500				200–500
Flux estimate (t/year)	1555 ± 753	No data	No data	4080	14850 ± 10450	1600 ± 300		6400 ± 1100		160 ± 70
Flux estimate size range (μm)	>100			<300	40–900	50–2000		No data		>200
Flux peak (μm)	250 ± 40	210–330		50–100	50–70	200–250		0–50		265 ± 92
CSs I-types (%)	2.2	5.0	3.0	4.1	27.7	2.1	5.9	No data	0.0	5.5
CSs G-types (%)	2.3	2.1	1.0	0.0	0	1.0	1.8		0.0	3.5
CSs S-types (%)	95.6	95.7	95.0	95.9	72.3	96.9	92.4		100	90.6
CSs S-types: PO (%)	16.9	31.6	9.5	68.5	35.9	24.0	38.9		19.0	25.1
CSs S-types: BO (%)	19.9	20.1	29.5	13.7		42.7	18.0		48.0	50.1
CSs S-types: CC (%)	51.6	23.1	20.9	13.7		12.5	21.3		33.0	7.5
CSs S-types: V (%)	7.5	18.0	35.2		36.4	17.7	14.2		0.0	7.9

[a]Value decreases decreasing significantly with increasing particle size.

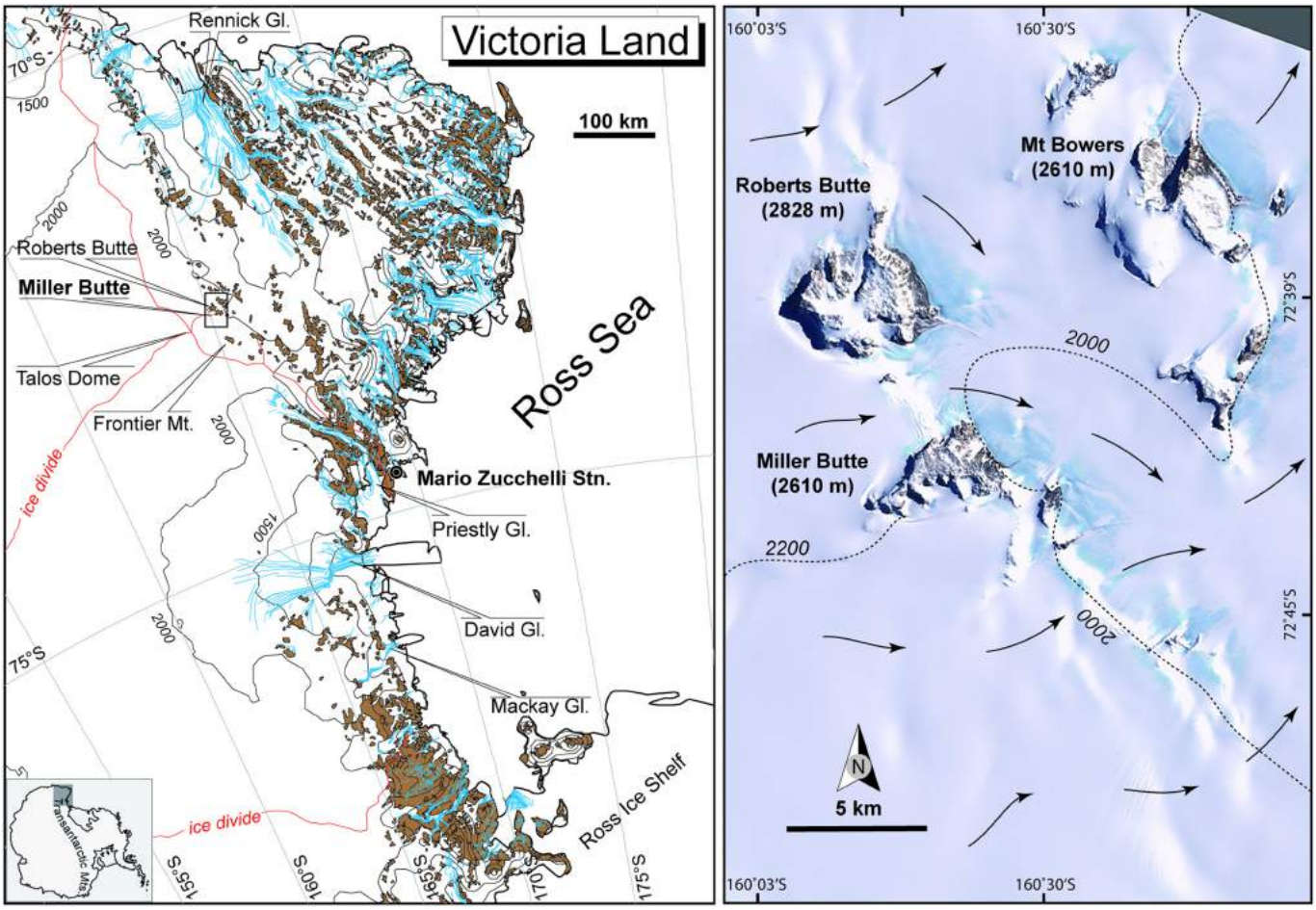

Figure 1. Location maps of Miller Butte (modified after Folco et al. (2002) and D'Orazio et al. (2006)). (a) Sketch map of Victoria Land (Antarctica) showing location of Miller Butte (~72°42′S, 160°17′E) and the Italian Mario Zucchelli station, ~250 km due SSE. Brown area represents exposed bedrock, blue lines show ice flow, and red lines mark ice-divides. Solid black rectangle identifies the area of the satellite image in (b). (b) LANDSAT TM satellite image of the Miller Butte area. Black arrows show ice flow and dashed lines are contour lines.

Antarctic Ice Sheet in a regional northward flow during a former high stand in the Cenozoic (van der Wateren et al., 1996). Exposure ages of surface in the region obtained through ^{10}Be, ^{26}Al, and ^{3}He cosmogenic nuclide analyses range from 2.3 (Mount Bowers; a few kilometers due north of Miller Butte; Figure 1b; van der Wateren et al., 1996, 1999) to 4 million years (Frontier Mountain; ~30 km due SSW of Miller Butte; Rochette et al., 2008; Welten et al., 2008). Cracks, eroded joints, and weathering pits on this surface are filled with a gritty loose sediment (regolith) derived from the erosion of the granitic bedrock, providing the geological setting for the accumulation of cosmic dust fallout (Rochette et al., 2008).

Large, tens of meters long, snow drifts occurring locally on the summit plateau indicate dominant winds blowing from the south. Wind direction and strength data (over 58,000 records) from the Antarctic automated Weather Station Paola at Talos Dome (see supporting data set "wind data"; ~40 km due ESE of Miller Butte; Figure 1a) recorded since 2003 consistently indicate dominant southern winds with 77% of the events from the southern quadrants. Their average wind speeds is around 9–10 knots (~4–5 m/s), maximum wind speeds around 40 knots, with 81% of the recorded events with moderate to weak winds with speeds comprised between 2 and 16 knots (1 to 8 m/s, respectively), 9% of calm and 10% of strong winds (>16 knots) up around 40 knots (21 m/s). The characteristics of the TAM65 micrometeorite trap are similar to earlier micrometeorite traps previously described by Rochette et al. (2008). In particular, the TAM65 trap consists of a 5–10-cm-thick layer of a gritty loose regolith derived from the erosion of the local bedrock, which acts as a trapping substrate for infalling particulate. The trap occurs on the stoss side of a glacial

Figure 2. Geomorpholoigcal features of Miller Butte (~72°42′S, 160°17′E; Antarctica). The butte consists of felsic granoid rocks of the Granite Harbour Intrusive Complex. (a) The western/plateau side of the butte (aerial view from the south). The peneplaned summit plateau at an average altitude of 2,600 m above sea level is 300–400 m above the regional ice level. (b) Grazing view from the north of the gently undulated, nearly horizontal summit plateau. Note the subparallelism with the joint system visible on the northern cliff of the butte. (c) Oblique aerial view from the north of the top surface showing barren glacially eroded surfaces (polish) and patches of rockfields. The approximate location of the sampled micrometeorite trap (TAM65) is arrowed.

bump at the top of the butte, which gently dips southward (Figure 3a). This surface is a stepped glacial polish, as a result of glacial erosion of the pervasively jointed structure of the granitic body. Blockfields lay locally on the glacial polish. The TAM65 sample was recovered from a layer of regolith accumulated between the upglacier (and upwind) side of an erosion step and a blockfield, as shown in Figures 3b and 3c. The sediment in the layer is vertically wind-sorted with inverse grading from pebble-gravel to dust. Grain size decreases with depth, namely, from centimeter- to millimeter-sized particles at the top to less than 65 mm toward the bottom. The finer fraction is usually dark grey due to the occurrence of abundant clay, tephra, and micrometeorites, and contrasts with the pale color of the larger size fraction dominated by granitic particles.

The TAM65 regolith sample—extracted as a <5-mm size fraction—was collected using trowels, brush, and sieve from a regolith patch measuring ~70 × ~70 cm (Figure 3b) with a local thickness of about 5 cm. Care was paid to gently sweep clean and collect the fines at the bottom of this layer down to the bedrock polished surface. A total of ~15 kg of regolith was collected, bagged, and brought to Mario Zucchelli station (the

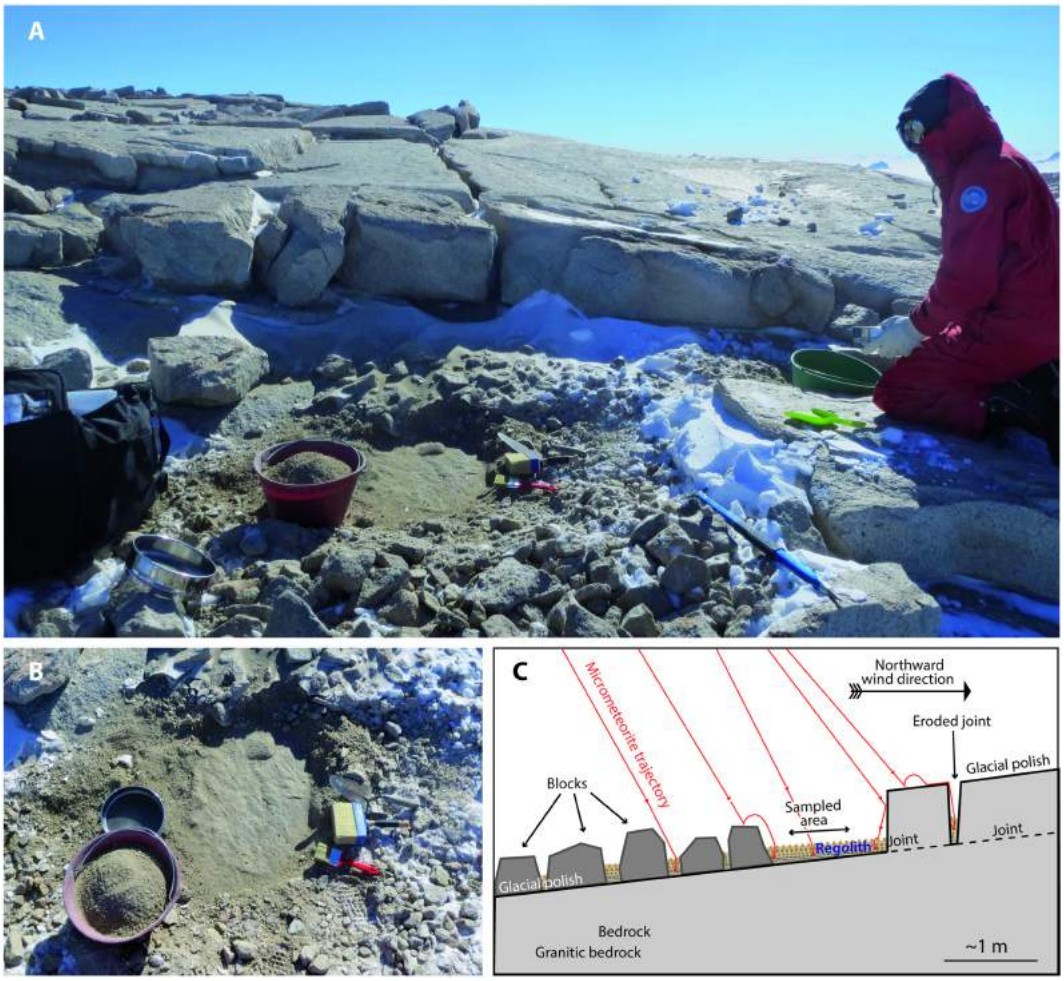

Figure 3. Field photos of the TAM65 micrometeorite trap sampled in this work from the summit plateau of Miller Butte. (a) Stepped glacial polish on the stoss and upwind bedrock side of a bedrock bump (looking northward). The erosion of local bedrock produces a gritty regolith which accumulates in between the bedrock step (downwind side) and a field of blocks (upwind side) giving rise to a thin layer of ~5–10 cm in thickness. (a) The sample was collected ~50 cm away from the step and block field. Scale: the stainless steel sieve is 20-cm diameter. (b) A close-up view of the sampled area measuring ~70 × 70 cm. (c) A schematic section of the micrometeorite trap, illustrating the trapping mechanism within the gritty regolith.

Italian Programma Nazionale delle Ricerche in Antartide Antarctic summer station) for preliminary curation, conditioning, and oversea shipping to our laboratories in Pisa.

3. Methods

For this study we collected 15 kg of loose sediment and investigated a subsample with a weight of 2,540 g. This was split into several size fractions (<63 μm [12 g], 63–100 μm [33 g], 100–200 μm [149 g], 200–400 μm [90 g], 400–800 μm [179 g], 800–2,000 μm [941 g], and >2,000 μm [1,138 g]) using a series of uncontaminated cascade sieves. Each size fraction was then passed through a fine-grained magnetic mineral separator (3 times per fraction), producing magnetic and nonmagnetic portions. For each size fraction (and mag/nonmag subdivision) either the entire separation or a subsampled aliquot was then searched in an exhaustive picking effort. We ensured that each sample was searched completely by both researchers (MDS and LF), while also collecting particles with a range of optical properties (dark, irregular-shaped, rounded, smooth, fluffy, glassy, metallic, etc.) these efforts aimed to minimize the number of unpicked micrometeorites—thereby minimizing human biases affecting the collection effort.

All potential micrometeorites were imaged optically (external surfaces) and under BSE (back-scattered electron imaging for both their external and internal sectioned perspective).

3.1. Extraterrestrial Identification

Micrometeorite identification was based on well-established textural criteria (e.g., the presence of igneous rims, magnetite rims, and dehydration cracks, rounded to spherical particle morphologies) and geochemical properties (chondritic bulk compositions, Ni-bearing metal, and high CaO, Cr_2O_3 olivines) as defined in Genge et al. (2008). Micrometeorites were classified following the system of Genge et al. (2008) and applying the updated suggestion established in van Ginneken et al. (2017) (e.g., the additional classification of μPO-type particles, which consist of numerous subhedral olivine crystals, typically <10 μm in size and abundant small vesicles). These data were used to determine population statistics, including relative abundances of different micrometeorite subtypes.

In total we picked 1,643 micrometeorites, ranging in size between 100 and 1,500 μm. However, because partial searches were performed on the smaller (<400 μm) size fractions the total expected micrometeorite population accounting for the unpicked micrometeorites lies at 3,310 particles (>100 μm) among the 2,540 g of sediment.

3.2. Size Distribution

Following positive extraterrestrial identification, micrometeorite particle sizes were measured using the ImageJ software (Schneider et al., 2012). We analyzed their BSE external images to accurately characterize particle sizes. These data were used to calculate a whole-collection rank-size distribution (fitted against both a power law and an exponential function) and size distributions for each textural subtype of cosmic spherule.

3.3. Particle Densities

We also calculated the densities for 57 cosmic spherules, with near-perfect spherical morphologies and within the size range 200–400 μm; this included two G-type spherules and 55 S-type spherules. Particle masses were weighed using a Mettler Toledo mass balance (model XP6/Z), with a precision of ±0.001 mg. Particle diameters were measured under SEM, using BSE imaging of their exterior surfaces, as described above; these measurements have a precision of ±10 μm. Particle volumes were then calculated using the volume of an oblate spheroid equation ($v = 4/3\pi \bullet b^2 \bullet c$, where b and c are the semimajor and semiminor axes, respectively) and subsequently used to determine mass values for each particle.

3.4. Mass Flux Calculation

In addition, we calculated a mass flux estimate of cosmic dust falling to Earth per year, for comparison against existing estimates. This was achieved by estimating the total extraterrestrial mass preserved in the TAM65 trap (converting the micrometeorite abundance data into mass data, using both empirical [self-derived] and literature density constraints) and then upscaling this mass flux to a global flux (based on the area size of the TAM65 trap and the global surface area) and finally dividing our upscaled mass value by the estimated age of the micrometeorite collection (using both the min and max age limits). Finally, we calculate the relative abundances of well-defined textural features previously identified in the literature including the presence of Fe-Ni metal and metal-sulfide beads (Genge & Grady, 1998), cumulate layering textures (Genge et al., 2016), and tailed or dumbbell-shaped morphologies (among melted cosmic spherules (Suttle et al., 2018)).

4. Results

4.1. Micrometeorite Abundance

We picked 1,643 micrometeorites, as well as 69 microtektites and 1 meteorite fragment (containing a thick fusion crust and identified as an equilibrated high-metamorphic grade ordinary chondrite). However, this "empirical" population does not represent the entire micrometeorite abundance expected within the investigated sediment load. This is because we did not search the entire sediment in each size fraction (the smaller size fractions requiring subsampling to make extraction feasible). Thus, a "synthetic" population of additional micrometeorites was required. This synthetic population accounts for the remaining particles hidden within the unsearched sediment and which would have been found had we continued to search the entire sample of each size fraction.

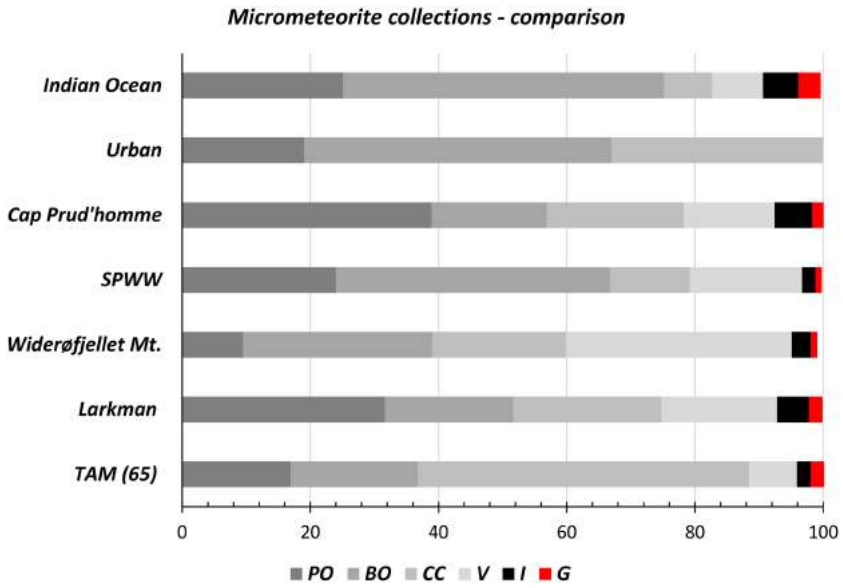

Figure 4. Cosmic spherule population statistics at TAM65 and comparison against some other established collections.

To model the synthetic population, we used the empirical population as a template. We randomly cloned some of the picked particles to generate synthetic duplicates. The number of synthetic particles required was determined, based on the mass ratio of searched-to-unsearched sediment in each size fraction. As a first-order approximation, the number of synthetic particles is approximately equal to the number of picked particles (the generation of the synthetic population and the TAM65 population statistics are shown in the supporting data, sheets "A" to "C").

Because the synthetic particles are clones, they have identical properties (size, texture, and composition) as their real counterparts. This process ensured that we were able to accurately model TAM65's population statistics, size distribution, and other features of the collection. Similar procedures were used by Taylor et al. (2007, 2012) and Suavet et al. (2009), where additional descriptions are also given. After extrapolation we estimate 3,310 particles among the 2,540 g of studied sediment.

4.2. Micrometeorites by Textural Type

Unmelted and scoriaceous particles represent 7% of the total collection at a ratio of 1:14 (0.07—unmelted micrometeorites to cosmic spherules). Fine-grained precursors are overwhelmingly dominant (~75%) among the unmelted particles, consistent with the conclusions of Taylor et al. (2012).

Among the cosmic spherule population (Figure 4), both I and G types occur in equal proportions (2.2–2.3%), while S-types make up the remaining 95.6%. S-types are subdivided based upon their quench textures into porphyritic (PO; 16.9%), barred olivine (BO; 19.9%), cryptocrystalline (CC; 51.6%), and vitreous (V; 7.5%). Splitting further, the PO group is composed of "normal" PO spherules (12.3%) containing "large" (>10μm) euhedral olivine crystals and μPO (3.4%) dominated by many smaller equant olivine crystals (<10 μm) as well as containing abundant vesicles. Collectively, among the whole porphyritic group 30.0% are relict grain bearing, containing residual crystals which survived atmospheric entry unmelted.

We also elected to further subdivide the CC class into "microcrystalline" (30.5%)—containing localized regions with a barred texture as well as regions lacking bars and dominated by randomly orientated olivine and magnetite crystallites, CC-normal (13.2%)—containing submicron olivine and magnetite dendrites with no evidence of barred textures and CC-turtleback (7.4%) composed of multiple crystalline domains whose boundaries present a *stitched* texture generated by crystal growth from the surface inward and generally lacking oxidized Fe (in the form of magnetite; Genge et al., 2008). These subdivisions better reflect the transitional nature between BO-CC-V subtypes and address somewhat the subjective problems of micrometeorite classification by texture.

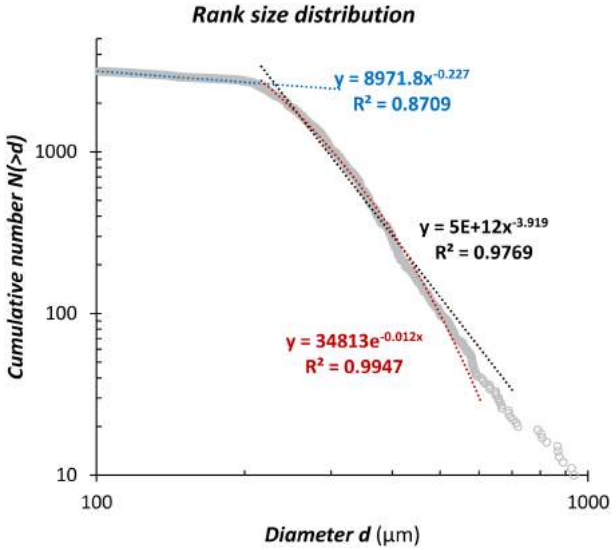

Figure 5. Rank-size distribution for the TAM65 micrometeorite collection. This population (naturally) segments into a short head and long tail. Each segment is fitted against numerical models (blue = power law relationship for small size fractions [100–200 μm], black = power law relationship for the main population [200–700 μm], and red = exponential relationship [200–700 μm]). Micrometeorites >700 μm were not fitted to a model due to the limited number of particles ($n = 22$).

We also provide the first relative abundance data for several unusual features found in S-type cosmic spherules:

- Approximately 3.2% of the S-types are tailed; their shapes deviate significantly from the ideal spherical morphology, owing to the presence of a single tapering extension of silicate melt. Tailed micrometeorites were first reported by Taylor et al. (2000) (Figure 5) and later found among the TAM collection (Suavet et al., 2009, Figure 6i; Suttle et al., 2018); their formation mechanism is unresolved.
- Metal beads, formed by the segregation of immiscible Fe–Ni metal (or Fe–Ni sulfides) from silicate melt (Genge & Grady, 1998), were found in 20.4% of S-type cosmic spherules.

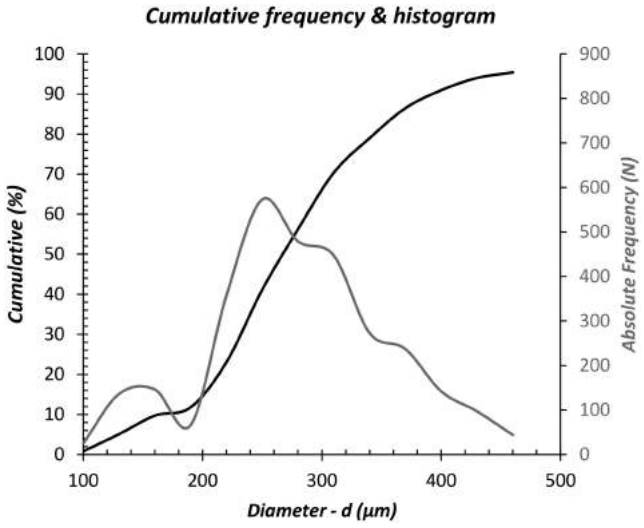

Figure 6. Cumulative frequency and frequency distribution plot for the TAM65 micrometeorite collection illustrating that the most common micrometeorite size is approximately 250 μm, consistent with data from other collections. We also note the clear break in the frequency distribution, and clearly distinct population occurring at sizes <200 μm.

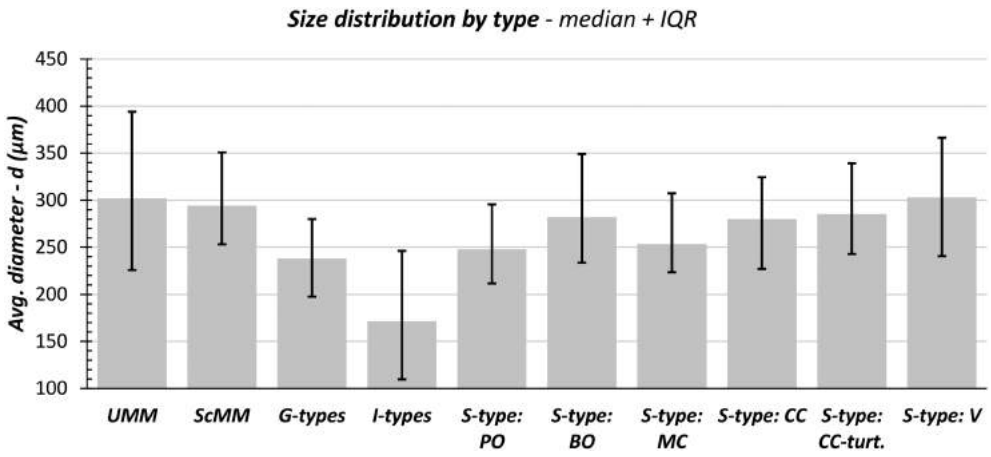

Figure 7. Size distribution by micrometeorite type, median (marked by the tops of each grey bar), and interquartile range (marked by black lines), demonstrating a lack of variation between average particle size, size range, and textural subtype. However, unmelted micrometeorites and I-types may show minor differences in their average abundances, preferential toward larger (~200–400 μm) and smaller sizes (120–250 μm), respectively.

- Hollow spherules occur at a frequency of 1.6% and contain a single large off-center vesicle (>40 vol %). They were first reported in Folco and Cordier (2015) and later suggested by Genge (2017) to form by rapid spin rates (of several thousand radians per second), potentially representing immature dust, recently released from their parent body, and whose fast rotation have not yet been slowed by magnetic dampening.

4.3. Size Distribution

We calculated a rank-size distribution for the TAM65 micrometeorite trap (Figure 5), displaying the cumulative number of micrometeorites greater than a given diameter. Rank-size distributions are appropriate where the studied population varies significantly in scale, for example over >2 orders of magnitude. In most situations rank-size distributions follow either a power law relationship (appearing as a straight line in log-log plots) or an exponential function (appearing as a concave curved line on log-log plots). The size distribution for TAM65 is segmented, showing a short head and a long tail, both with distinctly different slopes. The main population, between 200 and 700 μm, is fitted against both a power law (with a slope of −3.91, $R^2 = 0.977$) and an exponential (with an exponent of −0.012, $R^2 = 0.995$); meanwhile, the small size fractions (100–200 μm) are fitted against a power law with a slope of −0.227 ($R^2 = 0.871$). For micrometeorites >700 μm we did not fit a line-of-best-fit function since they number only 22 particles—insufficient for a meaningful slope fit.

4.4. Cumulative Frequency and Frequency Distribution (Figure 6)

Micrometeorite abundance peaks at 250 μm (±40 μm), consistent with data from other collections (Table 1; 210–330 μm (Genge et al., 2018), 200–250 μm (Taylor et al., 1998, 2000), and 265 μm [±92 μm] (Prasad et al., 2013)). Meanwhile, abundances <200 μm have a distinct abundance profile which appears unrelated to the larger size fractions.

4.5. Size Distribution by Type (Figure 7)

No significant size differences are observed among cosmic spherules of the S-type textural subgroups. For unmelted and scoriaceous micrometeorites, they are slightly more common at larger sizes (230–390 μm) than the average value (250 μm), while I-type cosmic spherules tend to be slightly more common among the smaller size fractions (110–240 μm).

4.6. Measurement of Cosmic Spherule Bulk Density

The two G-type spherules we measured have bulk density values between 5,000 and 5,800 kg m^{-3}. In contrast, the 55 S-type spherules have bulk densities between 1,100 and 4,200 kg m^{-3} with averages of 2,700, 2,700, and 2,300 kg m^{-3}—mean, median, and mode, respectively. For reference the density of quartz lies

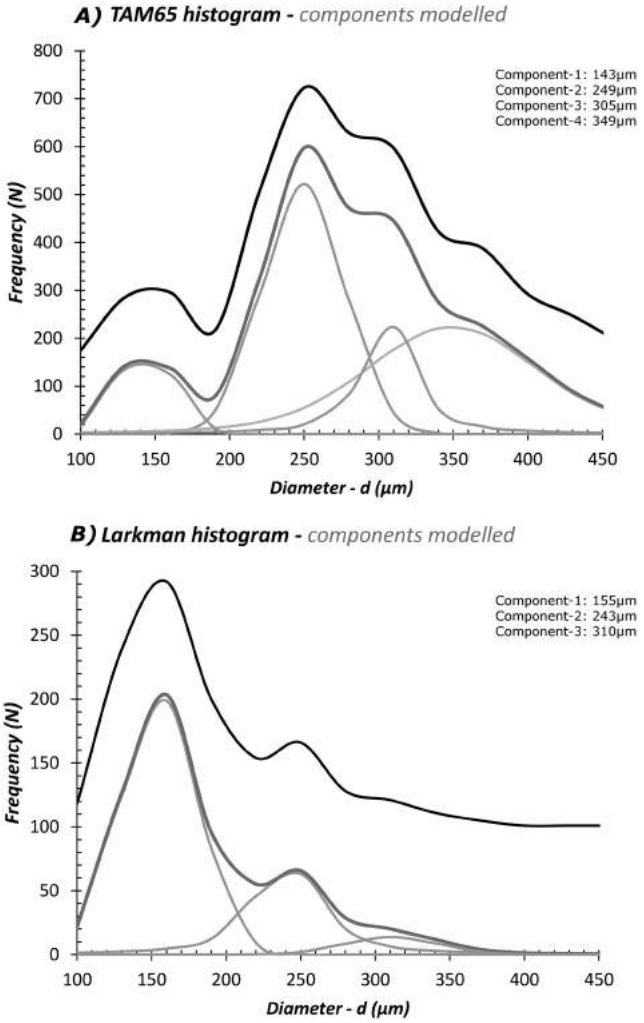

Figure 8. The micrometeorite flux presented as frequency distribution plots for both the (a) TAM65 and (b) Larkman Nunatak sites, demonstrating that the cosmic dust flux does not have a simple normal distribution centered on a single peak. This could suggest that the micrometeorite flux sampled at these sites is composed of several dust sources with distinct size distributions. Modeling of these two sites produces similar component peaks, strengthening the argument that we are resolving a true signal of the micrometeorite flux, although the relative contributions of each component are not the same at each site. Notably these shared peaks are located at ~150, 247, and 307 µm. This could correspond to different parent bodies (e.g., hydrated versus anhydrous) or to different components of parent bodies (e.g., matrix versus chondrules).

at ≃2,650 kg m^{-3} and olivine at ≃3,300 kg m^{-3}. Previous literature bulk density measurements of S-type spherules by Kohout et al. (2014) arrived at densities between 2,900 and 5,600 kg m^{-3} with mean averages of 3,200 kg m^{-3}. Similarly, Taylor et al. (2011) calculated the densities of 109 micrometeorites using modeled volumes from µCT data and arrived at bulk densities of 2,900 kg m^{-3} (±1,100 kg m^{-3}).

4.7. Micrometeorite Mass Within the TAM65 Trap

To estimate the mass of cosmic dust preserved within the TAM65 trap we must make several approximations. First, to calculate the mass of each micrometeorite we assume that all particles are perfect spheres with density values specific to each particle type. We use densities of 2,700 kg m^{-3} for S-type cosmic spherules (our own data; section 4.6), 5,400 kg m^{-3} for G-types (our own data; section 4.6), 5,000 kg m^{-3} for I-types (average data from Feng et al. (2005)), and 1,400 kg m^{-3} for unmelted and scoriaceous particles (average data from Kohout et al. (2014)). Thus, summing the mass of each individual micrometeorite (picked and inferred) gives a mass for the "recovered" micrometeorites at 0.295 g. This accounts for all micrometeorites within the investigated sediment mass (2,540 g, although only 1,403 g of this sediment have grain sizes <2,000 µm and was therefore *micrometeorite-bearing*). However, the TAM65 trap contained ~15 kg of sediment in total; thus, upscaling for the whole extraterrestrial micrometeorite mass within the trap gives a mass of 1.772 g (equivalent to ~1 g of cosmic dust per 4,750 g of sediment with grain sizes <2,000 µm).

The above mass estimate considers only micrometeorites with sizes >100 and <2,000 µm, while there are unlikely to be many more particles larger than 2,000 µm; a nonnegligible mass of extraterrestrial dust may be present in the <100-µm sediment fraction. Quantifying this missing micrometeorite mass is difficult and must rely on extrapolation of our calculated size distribution for the smaller size range (100–200 µm) downward. Such an inference may be reasonable down to perhaps 50 µm. However, below this point the abundance of micrometeorites is poorly studied and we therefore deem it unreasonable to continue extrapolation to even smaller sizes. We estimate that between 50 and 100 µm an additional 537 particles are likely to have been present and that their combined mass would add just 2.02E − 03 g of extraterrestrial mass to our budget's calculations (readers are directed to our supporting data file, sheet "D" where the small mass contribution calculations are shown).

5. Discussion

5.1. Distinct Sources Compose the Micrometeorite Flux (Figure 8)

In previous studies, authors have calculated a power law fit and used the resulting linear slope value to evaluate their micrometeorite collection with respect to sampling effort, accumulation dynamics, and weathering biases as well as attempting to resolve the *primary extraterrestrial signal*, that is, the size distribution of the cosmic dust flux reaching Earth (Taylor et al., 1998, 2000, and many studies thereafter; Table 1). Steep slopes (high coefficients) represent collections with proportionally fewer large micrometeorites, while shallow slopes (low coefficients) reflect collections dominated by large micrometeorites. The South Pole Water Well (SPWW) rank-size distribution, calculated using a power law distribution fit between ~200 and 700 µm, yielded slope values between −5.1 and −5.2. This has since been regarded as the unbiased size distribution of the near-Earth dust flux in the *present era*, not otherwise affected by weathering removal or other accumulation artifacts (Taylor et al., 2000).

In contrast, slope functions for older subaerial Antarctic weathering traps (e.g., TAM and the newly described Widerøefjellet, Sør Rondane Mountains collection [Goderis et al., 2019]) as well as moraine deposits (at Larkman Nunatak; Genge et al., 2018) tend to have shallower slopes. The TAM65 collection reported here has a slope of −3.9 ($R^2 = 0.98$), Widerøefjellet has a slope of −4.4 (R^2 =0.92; Goderis et al., 2019) while Larkman Nunatak has a published slope of −5.3 ($R^2 = 0.99$); however, this is true over only a short section of the distribution (210–300 μm). Instead, a power law function fitted to the entire reported range (~60–440 μm) produces a slope function of −3.0 ($R^2 = 0.92$). Thus, these older collections appear to have an overabundance of larger particles when compared to the blue-ice SPWW collection. However, it is also apparent that all micrometeorite collections with published (rank-)size distribution data (including the SPWW) show a shallowing of the slope toward their head region, representing a progressive decrease in the relative abundance of smaller particles at a rate inconsistent with that predicted by a simple power law. This may be expressed either as a gradual curve as in the case of the Widerøefjellet (Goderis et al., 2019, Figure 4) and Larkman (Genge et al., 2018, Figure 3) collections or a more abrupt change, causing a clear segmentation of the size distribution, as in the case of TAM65 (Figure 5) and the SPWW (Taylor et al., 1998, Figure 2).

This apparent overabundance of large micrometeorites (beyond that predicted by the power law fit) and observed as a change in the slope profile of micrometeorite rank-size distributions cannot be a terrestrial artifact since it is observed across multiple micrometeorite collections, recovered from widely different deposits (Antarctic ice, moraine, and weathering pits). Instead, this trend most likely represents a true feature of the dust flux caused by multiple sources of dust each with a preferential and distinct size distribution. Thus, as a first-order approximation micrometeorite rank-size distributions suggest a bimodal contribution to the dust flux, composed of one main dust source dominating the flux at small size fractions (<100 μm) and another source dominating the flux at size fractions >200 μm, with the inflection position somewhere between 100 and 200 μm. To investigate this further we modeled potential component dust sources that could explain the frequency distribution data for the TAM65 and Larkman micrometeorite collections (Figure 8). We employed Voigt functions (a convolution of a Gaussian and Lorentzian distribution) with a damped least squares fitting method to match modeled peaks to local maxima in the size distribution data sets. Data processing was performed in the Fityk software package (see supporting data, sheet "G").

The TAM65 data (Figure 8a) are best explained by a four-part model, with component peaks centered at 143, 249, 305, and 349 μm, of which the 249-μm peak is dominant and therefore consistent with several previous estimates that have suggested the micrometeorite flux peaks around 250 μm (Table 1, row: "flux peak"). In contrast, the Larkman data (Figure 8b) are best explained by a three-component model, with peaks centered on 155, 243, and 310 μm. The striking similarity in the position of component peaks in the two independent collections (at approximately ~150, 247, and 307 μm) therefore strengthens the hypothesis that the micrometeorite flux is composed of several distinct components and that these are distinguishable in collection efforts at the Earth's surface.

For the Larkman collection, the authors previously suggested that winnowing may have preferentially affected the smallest size fractions and lowest density (unmelted and scoriaceous) particles, while weathering may have also removed some particles (Genge et al., 2018). Thus, these terrestrial overprint effects may explain why the relative contributions from each dust source do not match that observed at TAM65. Although, since the two sites sample different time frames it is also possible that the contributions from different dust sources vary over time. Naturally, this leads us to ask, what do these dust sources represent?

5.2. Explanations for the Different Dust Sources

We envisage three possible dichotomies that could be responsible for the two main size distributions of dust: (Blanchard et al., 1980) asteroidal versus cometary parent bodies, (Bones et al., 2019) hydrated versus anhydrous chondrites, or (Cordier & Folco, 2014) constituent components of chondrites: fine-grained matrix versus coarse-grained chondrules and CAIs. We outline below why these sources are possible.

(1) The parent bodies of micrometeorites and especially the relative contributions from asteroids versus comets remains a matter of debate. Although both asteroidal and cometary material are known among micrometeorite collections (Noguchi et al., 2015; van Ginneken et al., 2012) estimates of their relative contributions vary widely. For example, dynamical modeling of the Zodiacal cloud suggests that up to 85% of the cosmic dust reaching Earth may be cometary in origin, sourced from Jupiter family comets (Nesvorný et al.,

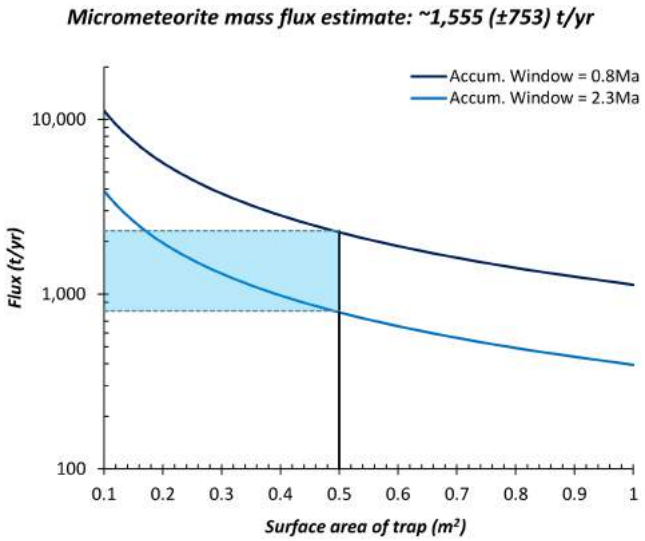

Figure 9. Mass flux estimate (in t/year) based on the TAM65 data. Our estimate varies significantly, dependent on two factors: the size and age of the collection site. Both variables are partially constrained, uncertainty arises due to the possible addition of particles by aeolian transport (as opposed to accumulation by direct infall only) and because the exact accumulation window of a micrometeorite site is not easily determined.

2010). Meanwhile petrological investigation of micrometeorites tends to conclude that asteroidal sources, from fine-grained hydrated CM, CR, and CI-like materials, are dominant (Kurat et al., 1994; Suttle et al., 2019; Taylor et al., 2012; van Ginneken et al., 2012). Finally, O-isotope data collated from multiple studies conclude that 20% of the dust flux is sourced from anhydrous inner solar system asteroids (ordinary chondrites and basaltic HED materials), while 60% are derived from primitive carbonaceous chondrite materials, including both CM/CO/CR/CI chondrites and cometary objects (Cordier & Folco, 2014; Goderis et al., 2019; Suavet et al., 2010; van Ginneken et al., 2017). The problems differentiating primitive asteroids and cometary material may reflect a possible continuum between these objects (Gounelle, 2011).

(2 and 3) Several impact experiments simulating the mechanical disruption and collisional release of dust from asteroid parent bodies have been performed (Durda and Flynn, 1999; Tomeoka et al., 2003; Flynn et al., 2009). High-speed impacts in a porphyritic olivine basalt target, simulating anhydrous stony meteorite fragmentation demonstrated that "fragments <100 μm in size were matrix while the majority of the largest fragments (>200 μm in size) were olivine [for example, representing disrupted chondrules]" (Durda and Flynn, 1999). Similar experiments have shown that anhydrous and hydrated chondrites fragment into preferentially finer (<100 μm) and coarser (>300 μm) size fractions, respectively (Tomeoka et al., 2003; Flynn et al., 2009). Data from these experiments therefore predict that different size fractions of the micrometeorite flux will preferentially sample different parent bodies. This has since been confirmed by empirical study (Cordier & Folco, 2014; Suavet et al., 2010; van Ginneken et al., 2012), and further suggests that we should expect at least one major inflection point in the size distribution of micrometeorite collections between 100 and 300 μm.

We therefore propose that the observed two component dust sources (divided around 150 μm) in Figure 8 represent either matrix versus chondrules, hydrated versus anhydrous parent bodies, or asteroids versus cometary material.

5.3. The Extraterrestrial Mass Flux of Cosmic Dust Reaching Earth (Figure 9)

Quantitative estimate of the flux of micrometeorites reaching the Earth' surface, namely, as a global mass addition in a given time frame, requires that the accumulation mechanism is well constrained and that no significant biases are introduced by secondary accumulation mechanisms—that is, micrometeorite loss due to erosion, loss due to weathering or effects introduced by recovery methods. Below we provide an estimate of the extraterrestrial mass flux arriving to Earth, based on the TAM65 data.

5.3.1. Accumulation Mechanism

Field observations reported above suggest that dominant mechanism through which most of the recovered micrometeorites accumulated in the TAM65 trap is direct infall and trapping in a wind-sorted sediment as shown in Figure 3c. Micrometeorites hit the gravel at the top of the gritty loose sediment layer and then migrate downward toward the finer sediment at the base.

Secondary accumulation from a larger collection surface is possible but likely not a major factor. The sediment is size-sorted, suggesting virtually no turbation of the sediment after its deposition due, for instance, to freeze-thaw cycles and water runoff, or aeolian pervasive reworking. Surface mass transport from the upglacier side of the trap seems to be improbable, as micrometeorites are unlikely to be transported (by saltation) once they are held within the sediment cover and sink downward toward into the trap. Surface mass transport along the clean polish surfaces downglacier of the trap is indeed possible as micrometeorite could be wind-drifted by saltation; however, an addition of micrometeorites to the sampled trap in this fashion would require winds blowing from the north, that is, directions opposite to the dominant winds in the area. Also, the sampled regolith was collected some tens of centimeters away from this polish surfaces in order to minimize the potential for this type of secondary contribution (Figure 3c). Note that the similarity between the size distribution, cumulative frequency, and frequency by type (particularly the lack of enrichment in denser types, like the I- and G-type cosmic spherules, and of depletion in lighter and more fragile types like the V-type cosmic spherules—including hollow spherules) of micrometeorites in the 100–700-μm size range between the TAM65 sample and other collections (Figure 4) points to negligible size and density sorting bias by wind or water. We thus suggest that most of the micrometeorites recovered in the TAM65 trap resulted from direct fall.

5.3.2. Periods Without Micrometeorite Accumulation

The accumulation of extraterrestrial dust at TAM65 will not have been continuous. Most notably, both wind and snow will have limited the preservation of infalling dust. Strong winds, sufficient to prevent micrometeorite-sized dust settling out of the air (suspension), will necessarily prevent accumulation. Considering a wind threshold shear velocity u ($u \sim [(\rho_p - \rho_{air}/\rho_{air})\, g\, D_p]^{1/2}$, where ρ_p and ρ_{air} are the density of the particle and of air, g is the gravitational acceleration, and D_p is the diameter of the particle) of approximately 2–5 m/s for a 200–800-μm-diameter micrometeorite with a density of ~2,900 kg/m^3 we speculate that winds with speeds of ~5–10 m/s would entrain micrometeorites in their flow in short-term suspension regimes, while strong winds in excess of tens of meters per second would make settling unlikely. Wind data from the closest Antarctic automated Weather Station Paola at Talos Dome (see supporting data set "Wind data") indicate that 10% of the time over the last 18 years (with measured activity) there were strong winds in excess of 16 knots (~8 m/s). This would imply a 10% underestimate in our global mass flux calculation (see below). Another variable that needs consideration is that winds, particularly those of moderate strengths, are not constant, therefore increasing the likelihood of settling; thus, our 10% underestimate due to wind action can be considered an upper limit.

In addition, when the trap's surface is covered by snow, cosmic dust could not be preserved. Grains will become trapped in the overlying snow and can either be removed by strong winds as the snow is drifted away or settle in the trap upon snow melting/sublimation. Genge et al. (2018) noted that the same limitation effects the Larkman Nunatak collection site and indeed we suggest that the action of winds removing surface material and snow cover preventing infalling dust are variables whose effects are both impossible to accurately quantify (with respect to their effect on micrometeorite accumulation over long durations) and are likely to affect all Antarctic surface-based micrometeorite collections to similar degrees. Sites such as Concordia and the SPWW which preserve micrometeorites in recent snow and older blue ice will have been subject to the same or indeed more extreme erosive events during their formation.

5.3.3. Micrometeorite Loss by Weathering

The above statistical similarities also point to a negligible micrometeorite decay due to weathering, at least in the size fraction >200 μm, as weathering acts selectively depending on composition (e.g., silicate S-type versus metallic I-type cosmic spherules; van Ginneken et al., 2016). The weathering style in the TAM micrometeorite traps is well-characterized (van Ginneken et al., 2016). Here weathering leads to the formation of salts (primarily jarosite) which encrust micrometeorites, while dissolution textures are also common and attack the external surfaces of particles, moving inward. However, four out of eight S-type cosmic spherules studied by Suavet et al. (2011) were found to have inverse polarity magnetic fields (suggesting arrival dates to Earth

prior to the most recent magnetic reversal event, that is, older that ~0.78 Ma). In addition, these spherules were found to be virtually devoid of weathering features, attesting to slow weathering rates at Miller Butte. We thus conclude that the loss of micrometeorites in the TAM65 micrometeorite trap due to weathering is negligible within the time scale of 1–2 Ma.

5.3.4. Age of the Trap

Like all the other micrometeorite traps from the TAM, TAM65 contains microtektites. These have characteristic petrographic and geochemical composition of the 788.1 ± 2.8 ka (Jourdan et al., 2019) Australasian microtektites and provided information of the minimum collection age of the TAM micrometeorite traps in Victoria Land (Folco et al., 2008). This minimum age of the TAM65 trap is consistent with the minimum age of other micrometeorite traps from the Miller Butte summit plateau where cosmic spherules recording reverse polarity and therefore fell to Earth at least 0.78 Ma ago (Suavet et al., 2011), as well as ablation debris associated with a Tunguska-like impact over Antarctica ~480 ka ago (van Ginneken et al., 2010) have both been found. Also, the ^{10}Be exposure age of an analogue glacial surface on Roberts Butte 6 km due north is 2.3 Ma (van der Wateren et al., 1996). Thus, the age of the TAM65 trap is constrained to be older than ~0.8 Ma and younger than 2.3 Ma.

5.3.5. Global Mass Flux to Earth's Surface (Figure 9)

cWe previously estimated a total mass of 1.772 g for the entire micrometeorite budget within the TAM65 trap (section 4.6). Assuming negligible secondary effects (accumulation or loss by terrestrial processes; sections 5.3.1–5.3.3) and 100% efficiency in micrometeorite recovery, we estimate a total mass flux of cosmic dust to Earth between 803 and 2,308 t/year. This estimate is based upon a collection area of 0.5 m^2 and an accumulation window between 0.8 and 2.3 Ma.

The uncertainty on the duration of the accumulation introduces a factor of 3 uncertainty in the flux estimate (additional information given in the supporting data, sheet "F"). Likewise, the surface area of the trap and the expected periods of no accumulation during strong winds (section 5.3.2) are difficult to quantify and this precludes a more precise flux estimate. Given the above limitations we conclude that the order-of-magnitude, time-averaged flux of cosmic dust (within the 100–2,000-μm size range) arriving on Earth over the last 0.8–2.3 Ma lies at approximately 1,555 (±753) t/year.

5.3.6. Comparison Against Existing Mass Flux Estimates

Most previous estimates of the micrometeorite mass flux (Table 1) have large uncertainties, owing to the loss of particles by weathering (Blanchard et al., 1980; Murrell et al., 1980; Peng & Lui, 1989), inefficiencies in magnetic collection and separation techniques (Blanchard et al., 1980; Murrell et al., 1980; Peng & Lui, 1989), low particle counts (Prasad et al., 2013; Yiou et al., 1989), poor age constraints (Murrell et al., 1980; Blanchard et al., 1980; Peng & Lui, 1989; Maurette et al., 1987, 1991; Prasad et al., 2013, 2018), or highly variable concentration processes (Maurette et al., 1991). Furthermore, previous measurements, whose accumulation windows (age) are better constrained, sample only the modern dust flux, with accumulation windows <50,000 years old (Table 1; Taylor et al., 1998, 2000; Duprat et al., 2007). In contrast, our estimate from the TAM65 trap provides a longer, time-averaged perspective on the cosmic dust flux—reflecting material deposited over much of the Quaternary period (2.58–0 Ma). However, despite significant differences in the accumulation window (collection age) and accumulation mechanism as compared to previous estimates, we arrived at a mass flux of ~1,500 t/year. This is consistent with most previous studies from both Greenland and Antarctica which sample significantly shorter accumulation windows (e.g., Maurette et al., 1987; Taylor et al., 1998, 2000; Duprat et al., 2007; Table 1). Additionally, our estimate is remarkably close the SPWW value in particular (1,600 ± 300; Taylor et al., 2000). Averaging four independent flux estimates (SPWW, Greenland, Concordia, and TAM65) gives a value of 3,400 t/year, with each lying between the range 1,500 and 6,500 t/year.

To our knowledge, there are only two (micrometeorite abundance based) mass flux estimates which have significantly different values. Yada et al. (2004) arrived at an estimate of 14,850 ± 10,450 t/year, whose upper limit is an order of magnitude larger than all other polar estimates and whose error margins approach 70% of the average value. This estimate therefore carries significant uncertainty and is most likely an overestimate. In contrast, researchers working on the Indian Ocean (deep-sea) collection suggested a much lower mass at just 160 (±70) t/year (Prasad et al., 2013) and later updated this to include contributions from unmelted particles, suggesting a value of 239 (±105) t/year (Prasad et al., 2018). However, deep-sea collections are strongly affected by terrestrial weathering (Murrell et al., 1980; Taylor et al., 2000). As such this significantly lower

estimate must be due to loss of particles by corrosion. Their reported proportions of geochemically resistant I and G-type cosmic spherules are higher than polar values (Taylor et al., 2000), while the silicate-dominated S-type cosmic spherules shown BSE images (Prasad et al., 2013, Figures 3–5) demonstrate clear evidence of etching, dissolution, and corrosion. Furthermore, fossil micrometeorite collections sampling limestone sediments formed on ancient seafloor have revealed that silicate-dominated micrometeorite rarely survive long exposure and are generally not preserved in sedimentary rocks (Suttle & Genge, 2017). Comparing estimates from polar collections to the Indian Ocean collection therefore suggests that as much as 90% of the initial micrometeorite content which fell to the seafloor has since been lost by corrosion.

Because there is now close agreement between several independent estimates for the cosmic dust mass flux to Earth, based on different collections with distinct accumulation mechanisms and accumulation windows, we tentatively conclude that the average flux of cosmic dust reaching the Earth's surface may not have varied significantly over the last 1–2 Ma (and therefore order-of-magnitude variations between terrestrial micrometeorite collections are not observed). This mass flux most likely lies between 1,500 and 6,500 t/year during the Quaternary period.

6. Conclusions

Micrometeorites preserved in subaerial Antarctic sediments (ice, snow, moraine, and weathering traps) provide a natural sampling of the cosmic dust flux falling to Earth over the geological past. By investigating a single sediment trap we explored the time-averaged micrometeorite flux to over (much of) the Quaternary. This study provides a unique perspective on the micrometeorite flux, as compared to previous studies which are otherwise limited to significantly shorter accumulation windows. Despite of the significantly longer collection age, micrometeorite abundance and size distribution data for TAM65 are broadly consistent with four previous flux estimates based on polar micrometeorite collections—implying that the cosmic dust flux may have varied relatively little over the recent geological past.

We show that a detailed investigation of size distribution data can reveal distinct components contributing to the micrometeorite flux. As a first-order approximation the flux has a bimodal distribution, with peaks centered at approximately 145 and 250 μm. These peaks most likely reflect either asteroidal versus cometary, hydrated versus anhydrous, or fine-grained versus coarse-grained parent body components. Further investigation, analyzing a much larger population of unmelted micrometeorites at each size fraction could resolve this problem.

We also provide the first mass flux estimate from the TAM micrometeorite collection, based on cosmic dust abundance data, arriving at a value of 1,555 (±753) t/year. To better resolve this estimate, we will analyze additional sediment traps at Miller Butte and conduct local ^{10}Be exposure age dating. This will improve the upper age constraint for the TAM traps and form the basis of future science goals for the TAM micrometeorite collection.

Author Contributions

Both authors contributed equally to this project at each stage from inception, planning, data collection, data processing, interpretation, and writing of the manuscript.

Data Availability Statement

The supporting data used in this publication are available at Suttle (2019)—provided as a Dryad data set (https://doi.org/10.5061/dryad.1c59zw3rh).

Acknowledgments
Micrometeorite research at Pisa University is funded through grants MIUR: PNRA16_00029 *Meteoriti Antartiche* and PRIN2015 *Cosmic Dust*. The authors declare no conflicts of interest, financial or otherwise. We also acknowledge support by the University of Pisa grant PRA_2018_19.

References

Blanchard, M. B., Brownlee, D. E., Bunch, T. E., Hodge, P. W., & Kyte, F. T. (1980). Meteoroid ablation spheres from deep-sea sediments. *Earth and Planetary Science Letters*, *46*, 178–190. https://doi.org/10.1016/0012-821X(80)90004-7

Bones, D. L., Carrillo-Sánchez, J. D., Kulak, A. N., & Plane, J. M. (2019). Ablation of Ni from micrometeoroids in the upper atmosphere: Experimental and computer simulations and implications for Fe ablation. *Planetary and Space Science*. https://doi.org/10.1016/j.pss.2019.104725

Cordier, C., & Folco, L. (2014). Oxygen isotopes in cosmic spherules and the composition of the near Earth interplanetary dust complex. *Geochimica et Cosmochimica Acta*, *146*, 18–26. https://doi.org/10.1016/j.gca.2014.09.038

Dobrica, E., Engrand, C., Duprat, J. and Gounelle, M., 2010. A statistical overview of concordia Antarctic micrometeorites. *Meteoritics and Planetary Science Supplement*, *73* (Abstr.#5213).

D'Orazio, M., Folco, L., Welten, K. C., Caffee, M. W., Perchiazzi, N., & Rochette, P. (2006). Miller Butte 03002: A new rare iron meteorite (IID) from Antarctica. *European Journal of Mineralogy*, *18*, 727–738.

Duprat, J., Engrand, C., Maurette, M., Gounelle, M. and Kurat, G., 2004. Micrometeorites from central Antarctic snow: The CONCORDIA-Collection. *In 35th COSPAR Scientific Assembly* 35.

Duprat, J., Engrand, C., Maurette, M., Kurat, G., Gounelle, M., & Hammer, C. (2007). Micrometeorites from central Antarctic snow: The CONCORDIA collection. *Advances in Space Research*, *39*, 605–611.

Duprat, J., Maurette, M., Engrand, C., Matraj, G., Immel, G., Hammer, C., et al. (2001). An estimation of the contemporary micrometeorite flux obtained from surface snow samples collected in central Antarctica. *Meteoritics and Planetary Science Supplement*, *36*, A52.

Feng, H., Jones, K. W., Tomov, S., Stewart, B., Herzog, G. F., Schnabel, C., & Brownlee, D. E. (2005). Internal structure of type I deep-sea spherules by X-ray computed microtomography. *Meteoritics & Planetary Science*, *40*, 195–206. https://doi.org/10.1111/j.1945-5100.2005.tb00375.x

Folco, L., Capra, A., Chiappini, M., Frezzotti, M., Mellini, M., & Tabacco, I. E. (2002). The Frontier Mountain meteorite trap (Antarctica). *Meteorit. Planet. Sci.*, *37*, 209–228.

Folco, L., & Cordier, C. (2015). Micrometeorites. EMU Notes in Mineralogy. In M. R. Lee & H. Leroux (Eds.), *Planetary Mineralogy*, *Edition: European Mineralogical Union, The Mineralogical Society of Great Britain and Ireland* (Vol. 15, Chap. 9, pp. 253–297). London: European Mineralogical Union. https://doi.org/10.1180/EMU-notes.15.9

Folco, L., Rochette, P., Perchiazzi, N., d'Orazio, M., Laurenzi, M. A., & Tiepolo, M. (2008). Microtektites from Victoria Land Transantarctic Mountains. *Geology*, *36*, 291–294. https://doi.org/10.1130/G24528A

Ganovex Team (1987). Geological map of North Victoria land, Antarctica, 1: 500,000— explanatory notes. *Geologisches Jahrbuch B*, *66*, 7–79.

Genge, M. J. (2017). Vesicle dynamics during the atmospheric entry heating of cosmic spherules. *Meteoritics & Planetary Science*, *52*, 443–457. https://doi.org/10.1111/maps.12805

Genge, M. J., Engrand, C., Gounelle, M., & Taylor, S. (2008). The classification of micrometeorites. *Meteoritics & Planetary Science*, *43*, 497–515. https://doi.org/10.1111/j.1945-5100.2008.tb00668.x

Genge, M. J., & Grady, M. M. (1998). Melted micrometeorites from Antarctic ice with evidence for the separation of immiscible Fe-Ni-S liquids during entry heating. *Meteoritics & Planetary Science*, *33*, 425–434. https://doi.org/10.1111/j.1945-5100.1998.tb01647.x

Genge, M. J., Larsen, J., van Ginneken, M., & Suttle, M. D. (2017). An urban collection of modern-day large micrometeorites: Evidence for variations in the extraterrestrial dust flux through the Quaternary. *Geology*, *45*, 119–122. https://doi.org/10.1130/G38352.1

Genge, M. J., Suttle, M., & Van Ginneken, M. (2016). Olivine settling in cosmic spherules during atmospheric deceleration: An indicator of the orbital eccentricity of interplanetary dust. *Geophysical Research Letters*, *43*, 10–646. https://doi.org/10.1002/2016GL070874

Genge, M. J., van Ginneken, M., Suttle, M. D., & Harvey, R. P. (2018). Accumulation mechanisms of micrometeorites in an ancient supraglacial moraine at Larkman Nunatak, Antarctica. *Meteoritics & Planetary Science*, *53*, 2051–2066. https://doi.org/10.1111/maps.13107

Goderis, S., Soens, B., Huber, M. S., McKibbin, S., Ginneken, V. M., Debaille, V., et al. (2019). Cosmic spherules from Widerøefjellet. *Sør Rondane Mountains (East Antarctica) Geochimica et Cosmochimica Acta*. https://doi.org/10.1016/j.gca.2019.11.016

Gounelle, M. (2011). The asteroid–comet continuum: In search of lost primitivity. *Elements*, *7*, 29–34. https://doi.org/10.2113/gselements.7.1.29

Jolliff, B. L., Korotev, R. L., & Haskin, L. A. (1993). An iridium-rich iron micrometeorite with silicate inclusions from the Moon. The 24th Lunar and Planetary Conference (LPSC) – (abstr#94N16281)

Jourdan, F., Nomade, S., Wingate, M. T., Eroglu, E., & Deino, A. (2019). Ultraprecise age and formation temperature of the Australasian tektites constrained by $^{40}Ar/^{39}Ar$ analyses. *Meteoritics & Planetary Science*. https://doi.org/10.1111/maps.13305

Kohout, T., Kallonen, A., Suuronen, J. P., Rochette, P., Hutzler, A., Gattacceca, J., et al. (2014). Density, porosity, mineralogy, and internal structure of cosmic dust and alteration of its properties during high-velocity atmospheric entry. *Meteoritics & Planetary Science*, *49*, 1157–1170. https://doi.org/10.1111/maps.12325

Kurat, G., Koeberl, C., Presper, T., Brandstätter, F., & Maurette, M. (1994). Petrology and geochemistry of Antarctic micrometeorites. *Geochimica et Cosmochimica Acta*, *58*, 3879–3904. https://doi.org/10.1016/0016-7037(94)90369-7

Maurette, M., Jehanno, C., Robin, E., & Hammer, C. (1987). Characteristics and mass distribution of extraterrestrial dust from the Greenland ice cap. *Nature*, *328*, 699–702. https://doi.org/10.1038/328699a0

Maurette, M., Olinger, C., Michel-Levy, M. C., Kurat, G., Pourchet, M., Brandstätter, F., & Bourot-Denise, M. (1991). A collection of diverse micrometeorites recovered from 100 tonnes of Antarctic blue ice. *Nature*, *351*, 44–47. https://doi.org/10.1038/351044a0

Maurette, M., Pourchet, M., Bonny, P., De Angelis, M., & Siry, P. (1989). A new collection of micrometeorites, extracted from 100 tons of artificially melted blue ice, near Cap-Prudhomme in Antarctica. *In Lunar and Planetary Science Conference.*, *20*, 644–645.

Murrell, M. T., Davis, P. A. Jr., Nishiizumi, K., & Millard, H. T. Jr. (1980). Deep-sea spherules from Pacific clay: Mass distribution and influx rate. *Geochimica et Cosmochimica Acta*, *44*, 2067–2074. https://doi.org/10.1016/0016-7037(80)90204-5

Nakamura, T., Imae, N., Nakai, I., Noguchi, T., Yano, H., Terada, K., et al. (1999). Antarctic micrometeorites collected at the Dome Fuji Station. *Antarctic Meteorite Research*, *12*, 183–198.

Nesvorný, D., Jenniskens, P., Levison, H. F., Bottke, W. F., Vokrouhlický, D., & Gounelle, M. (2010). Cometary origin of the zodiacal cloud and carbonaceous micrometeorites. Implications for hot debris disks. *The Astrophysical Journal*, *713*. https://doi.org/10.1088/0004-637X/713/2/816/meta

Nesvorný, D., Vokrouhlický, D., Bottke, W. F., & Sykes, M. (2006). Physical properties of asteroid dust bands and their sources. *Icarus*, *181*, 107–144. https://doi.org/10.1016/j.icarus.2005.10.022

Nishiizumi, K., Arnold, J. R., Brownlee, D. E., Caffee, M. W., Finkel, R. C., & Harvey, R. P. (1995). Beryllium-10 and aluminum-26 in individual cosmic spherules from Antarctica. *Meteoritics*, *30*, 728–732. https://doi.org/10.1111/j.1945-5100.1995.tb01170.x

Noguchi, T., Ohashi, N., Tsujimoto, S., Mitsunari, T., Bradley, J. P., Nakamura, T., et al. (2015). Cometary dust in Antarctic ice and snow: Past and present chondritic porous micrometeorites preserved on the Earth's surface. *Earth and Planetary Science Letters*, *410*, 1–11. https://doi.org/10.1016/j.epsl.2014.11.012

Peng, H., & Lui Z. (1989). Measurement of the annual flux of cosmic dust in deep-sea sediments, The 52nd Annual Meeting of the Meteoritical Society, 24:315.

Peucker-Ehrenbrink, B. (1996). Accretion of extraterrestrial matter during the last 80 million years and its effect on the marine osmium isotope record. *Geochimica et Cosmochimica Acta*, *60*, 3187–3196. https://doi.org/10.1016/0016-7037(96)00161-5

Prasad, M. S., Rudraswami, N. G., de Araujo, A. A., & Khedekar, V. D. (2018). Characterisation, sources and flux of unmelted micrometeorites on Earth during the last ~50,000 years. *Scientific reports*, *8*(1), 8887. https://doi.org/10.1038/s41598-018-27158-x

Prasad, M. S., Rudraswami, N. G., & Panda, D. K. (2013). Micrometeorite flux on Earth during the last ~50,000 years. *Journal of Geophysical Research: Planets*, *118*, 2381–2399. https://doi.org/10.1002/2013JE004460

Rochette, P., Folco, L., Suavet, C., Van Ginneken, M., Gattacceca, J., Perchiazzi, N., et al. (2008). Micrometeorites from the transantarctic mountains. *Proceedings of the National Academy of Sciences*, *105*, 18,206–18,211. https://doi.org/10.1073/pnas.0806049105

Schmitz, B., Farley, K. A., Goderis, S., Heck, P. R., Bergström, S. M., Boschi, S., et al. (2019). An extraterrestrial trigger for the mid-Ordovician ice age: Dust from the breakup of the L-chondrite parent body. *Science Advances*. https://doi.org/10.1126/sciadv.aax4184

Schneider, C. A., Rasband, W. S., & Eliceiri, K. W. (2012). NIH Image to ImageJ: 25 years of image analysis, *Nature methods*, *9*:671-675, PMID 22930834. https://doi.org/10.1038/nmeth.2089.

Suavet, C., Alexandre, A., Franchi, I. A., Gattacceca, J., Sonzogni, C., Greenwood, R. C., et al. (2010). Identification of the parent bodies of micrometeorites with high-precision oxygen isotope ratios. *Earth and Planetary Science Letters*, *293*, 313–320. https://doi.org/10.1016/j.epsl.2010.02.046

Suavet, C., Gattacceca, J., Rochette, P., & Folco, L. (2011). Constraining the terrestrial age of micrometeorites using their record of the Earth's magnetic field polarity. *Geology*, *39*, 123–126. https://doi.org/10.1130/G31655.1

Suavet, C., Rochette, P., Kars, M., Gattacceca, J., Folco, L., & Harvey, R. P. (2009). Statistical properties of the Transantarctic Mountains (TAM) micrometeorite collection. *Polar Science*, *3*, 100–109. https://doi.org/10.1016/j.polar.2009.06.003

Suttle, M.D., Folco, L., Gemelli, M., Genge M., & Larsen, J. (2018). The formation of tailed cosmic spherules: Metal bead loss in S-type micrometeorites. Space dust and debris in the vicinity of the Earth - Royal Astronomical Society Specialist Meeting, 09/11/2018.

Suttle, M. D., Folco, L., Genge, M. J., Russell, S. S., Najorka, J., & van Ginneken, M. (2019). Intense aqueous alteration on C-type asteroids: Perspectives from giant fine-grained micrometeorites. *Geochimica et cosmochimica acta*, *245*, 352–373. https://doi.org/10.1016/j.gca.2018.11.019

Suttle, M. D., & Genge, M. J. (2017). Diagenetically altered fossil micrometeorites suggest cosmic dust is common in the geological record. *Earth and Planetary Science Letters*, *476*, 132–142. https://doi.org/10.1016/j.epsl.2017.07.052

Suttle, M. D., van Ginneken, M., & Genge, M. J. (2015). Larkman Nunatak micrometeorites, a statistical study. 78th Annual Meeting of the Meteoritical Society, held July 27-31, 2015 in Berkeley, California. LPI Contribution No.1856, (Abstr.#5063).

Suttle, M. (2019). The extraterrestrial dust flux: Size distribution and mass contribution estimates inferred from the Transantarctic Mountain (TAM) micrometeorite collection, v2. *Dryad, Dataset*. https://doi.org/10.5061/dryad.1c59zw3rh

Taylor, S., Jones, K. W., Herzog, G. F., & Hornig, C. E. (2011). Tomography: A window on the role of sulfur in the structure of micrometeorites. *Meteoritics & Planetary Science*, *46*, 1498–1509. https://doi.org/10.1111/j.1945-5100.2011.01245.x

Taylor, S., Lever, J. H., & Harvey, R. P. (1998). Accretion rate of cosmic spherules measured at the South Pole. *Nature*, *392*(6679), 899–903. https://doi.org/10.1038/31894

Taylor, S., Lever, J. H., & Harvey, R. P. (2000). Numbers, types, and compositions of an unbiased collection of cosmic spherules. *Meteoritics & Planetary Science*, *35*, 651–666. https://doi.org/10.1111/j.1945-5100.2000.tb01450.x

Taylor, S., Matrajt, G., & Guan, Y. (2012). Fine-grained precursors dominate the micrometeorite flux. *Meteoritics and Planetary Science*, *47*, 550–564. https://doi.org/10.1111/j.1945-5100.2011.01292

Taylor, S., Matrajt, G., Lever, J. H., Joswiak, D. J., & Brownlee, D. E. (2007). Size distribution of Antarctic micrometeorites. *Dust in Planetary Systems*, *643*, 145–148.

Terada, K., Yada, T., Kojima, H., Noguchi, T., Nakamura, T., Murakami, T., et al. (2001). General characterization of Antarctic micrometeorites collected by the 39th Japanese Antarctic Research Expedition: Consortium studies of JARE AMMs (III). *Antarctic Meteorite Research*, *14*, 89–107.

Tomeoka, K., Kiriyama, K., Nakamura, K., Yamahana, Y., & Sekine, T. (2003). Interplanetary dust from the explosive dispersal of hydrated asteroids by impacts. *Nature*, *423*(6935), 60–62. https://doi.org/10.1038/nature01567

van der Wateren, F. M., Dunai, T. J., Van Balen, R. T., Klas, W., Verbers, A. L., Passchier, S., & Herpers, U. (1999). Contrasting Neogene denudation histories of different structural regions in the Transantarctic Mountains rift flank constrained by cosmogenic isotope measurements. *Global and Planetary Change*, *23*, 145–172. https://doi.org/10.1016/S0921-8181(99)00055-7

van der Wateren, F. M., Verbers, A. L. L. M., Luyendyk, B. P., Smith, C. H., Hofle, H. C., Vermeulen, F. J. M., et al. (1996). Glaciation and deglaciation of the uplifted margins of the Cenozoic West Antarctic rift system, Ross Sea, Antarctica. *Geologisches Jahruch Reihe B*, 123–156.

van Ginneken, M., Folco, L., Cordier, C., & Rochette, P. (2012). Chondritic micrometeorites from the Transantarctic Mountains. *Meteoritics & Planetary Science*, *47*, 228–247. https://doi.org/10.1111/j.1945-5100.2011.01322.x

van Ginneken, M., Folco, L., Perchiazzi, N., Rochette, P., & Bland, P. A. (2010). Meteoritic ablation debris from the Transantarctic Mountains: Evidence for a Tunguska-like impact over Antarctica ca. 480 ka ago. *Earth and Planetary Science Letters*, *293*, 104–113. https://doi.org/10.1016/j.epsl.2010.02.028

van Ginneken, M., Gattacceca, J., Rochette, P., Sonzogni, C., Alexandre, A., Vidal, V., & Genge, M. J. (2017). The parent body controls on cosmic spherule texture: Evidence from the oxygen isotopic compositions of large micrometeorites. *Geochimica et Cosmochimica Acta*. https://doi.org/10.1016/j.gca.2017.05.008

van Ginneken, M., Genge, M. J., Folco, L., & Harvey, R. P. (2016). The weathering of micrometeorites from the Transantarctic Mountains. *Geochimica et cosmochimica Acta*, *179*, 1–31. https://doi.org/10.1016/j.gca.2015.11.045

Welten, K. C., Folco, L., Nishiizumi, K., Caffee, M. W., Grimberg, A., Meier, M. M. M., & Kober, F. (2008). Meteoritic and bedrock constraints on the glacial history of Frontier Mountain in northern Victoria Land, Antarctica. *Earth Planetary Science Letters*, *270*, 308–315. https://doi.org/10.1016/j.epsl.2008.03.052

Yada, T., & Kojima, H. (2000). The collection of micrometeorites in the Yamato meteorite ice field of Antarctica in 1998. *Antarctic Meteorite Research*, *13*, 9.

Yada, T., Nakamura, T., Takaoka, N., Noguchi, T., Terada, K., Yano, H., et al. (2004). The global accretion rate of extraterrestrial materials in the last glacial period estimated from the abundance of micrometeorites in Antarctic glacier ice. *Earth, planets and space*, *56*(1), 67–79. https://doi.org/10.1186/BF03352491

Yiou, F., Raisbeck, G. M., & Jéhanno, C. (1989). Influx of cosmic spherules to the Earth during the last ~105 years as deduced from concentrations in Antarctic ice cores. *Meteoritics*, *24*, 344.

Zolensky, M., Bland, P., Brown, P., & Halliday, I. (2006). Flux of extraterrestrial materials. *Meteorites and the early solar system II*, 869–888.